Research Article | Vol. 7, No. 7 | 1 Jul 2017 | OPTICAL MATERIALS EXPRESS 2511
Optical Materials EXPRESS

Hafnia-yttria-alumina-silica based optical fibers with diminished mid-IR (>2 μm) loss

A. V. Kir'yanov,[1,2,6] S. H. Siddiki,[3] Y. O. Barmenkov,[1] S. Das,[3] D. Dutta,[3] A. Dhar,[3] A. V. Khakhalin,[4] E. M. Sholokhov,[4] N. N. Il'ichev,[5] S. I. Didenko,[2] and M. C. Paul[4,7]

[1]*Centro de Investigaciones en Optica, Loma del Bosque 115, Col. Lomas del Campestre, Leon 37150, Mexico*
[2]*National University of Science and Technology (MISIS), Leninsky Avenue 4, Moscow 119049, Russia*
[3]*Fiber Optics and Photonic Division, Central Glass & Ceramic Research Institute-CSIR, 196, Raja S.C. Mullick Road, Kolkata-700 032, India*
[4]*Physics Department, Lomonosov Moscow State University, Vorobyevy Gory, Moscow 119991, Russia*
[5]*A.M. Prokhorov General Physics Institute, Russian Academy of Sciences, Vavilov Street 38, Moscow 119991, Russia*
[6]*kiryanov@cio.mx*
[7]*paulmukul@hotmail.com*

Abstract: Fabrication details and basic characteristics of a set of novel multimode hafnia-yttria-alumina-silicate (HYAS) core-glass based fibers, one of which is co-doped with bismuth (Bi), for the mid-IR (> 2 μm) spectral range are reported. It is demonstrated that fibers of this type possess low fundamental loss in the spectral range beyond 2 μm, lowered by fewer times as compared to conventional silica-based ones, even at moderate (units of mol.%) co-doping with hafnium. This makes them attractive for versatile mid-IR applications. Furthermore, HYAS core-glass fiber co-doped with Bi is revealed to have all the signs of 'active' (fluorescing) Bi-related centers, thus being suitable for lasing/amplifying in the near-IR spectral range.

OCIS codes: (060.2290) Fiber materials; (160.2750) Glass and other amorphous materials; (300.6250) Spectroscopy, condensed matter.

References and links

1. D. L. Wood, K. Nassau, T. Y. Kometani, and D. L. Nash, "Optical properties of cubic hafnia stabilized with yttria," Appl. Opt. **29**(4), 604–607 (1990).
2. D. Neumayer and E. Cartier, "Materials characterization of ZrO_2-SiO_2 and HfO_2-SiO_2 binary oxides deposited by chemical solution deposition," J. Appl. Phys. **90**(4), 1801–1808 (2001).
3. S. Todoroki, K. Hirao, and N. Soga, "Origin of inhomogeneous linewidth of Eu^{3+} fluorescence in several oxide glasses," J. Appl. Phys. **72**(12), 5853–5860 (1992).
4. N. D. Afify, G. Dolba, C. Armellini, M. Ferrari, F. Rocca, and A. Kuzmin, "Local structure around Er^{3+} in SiO_2-HfO_2 glassy waveguides using EXAFS," Phys. Rev. B **76**(2), 024114 (2007).
5. J. K. Sahu, P. Dupriez, J. Kim, and A. J. Boyland. C. A. Codemard, J. Nilsson, and D. N. Payne, "New Yb:Hf-doped silica fiber for high-power fiber lasers," in *Conference on Lasers and Electro-Optics/Quantum Electronics and Laser Science and Photonic Applications Systems Technologies*, Technical Digest (CD) (Optical Society of America, 2005), paper CTuK1.
6. X. Yan, D. Su, H. Duan, and F. Zhang, "Preparation of SiOC/HfO_2 fibers from silicon alkoxides and tetrachloride hafnium by a sol–gel process," Mater. Lett. **148**, 196–199 (2015).
7. D. Benerjee, P. Das, R. Guin, and S. K. Das, "Nuclear quadrupole interaction at ^{181}Ta in hafnium dioxide fiber: Time differential perturbed angular correlation measurements and ab-initio calculations," J. Phys. Chem. Solids **73**(9), 1090–1094 (2012).
8. N. C. Das, N. K. Sahoo, D. Bhattacharyya, S. Thakur, N. M. Kamble, D. Nanda, S. Hazra, J. K. Bal, J. F. Lee, Y. L. Tai, and C. A. Hsieh, "Correlation between local structure and refractive index of e-beam evaporated (HfO_2–SiO_2) composite thin films," J. Appl. Phys. **108**(2), 023515 (2010).
9. E. M. Dianov, V. V. Dvoyrin, V. M. Mashinsky, A. A. Umnikov, M. V. Yashkov, and A. N. Guryanov, "CW bismuth bre laser," Quantum Electron. **35**(12), 1083–1084 (2005).
10. V. V. Dvoyrin, A. V. Kir'yanov, V. M. Mashinsky, O. I. Medvedkov, A. A. Umnikov, A. N. Guryanov, and E. M. Dianov, "Absorption, gain and laser action in bismuth-doped aluminosilicate optical fibers," IEEE J. Quantum Electron. **46**(2), 182–190 (2010).

#294703 https://doi.org/10.1364/OME.7.002511
Journal © 2017 Received 28 Apr 2017; accepted 23 May 2017; published 20 Jun 2017

Optical Materials EXPRESS

11. A. V. Kir'yanov, A. Halder, Y. O. Barmenkov, S. Das, A. Dhar, S. K. Bhadra, V. G. Plotnichenko, V. V. Koltashev, and M. C. Paul, "Distribution of bismuth and bismuth-related centers in core area of Y-Al-SiO_2:Bi fibers," IEEE J. Lightw. Technol. **33**(17), 3649–3659 (2015).
12. D. Ramirez-Granados, A. V. Kir'yanov, Y. O. Barmenkov, A. Halder, S. Das, A. Dhar, M. C. Paul, S. K. Bhadra, S. I. Didenko, V. V. Koltashev, and V. G. Plotnichenko, "Effects of elevating temperature and high temperature annealing upon state-of-the-art of yttia-alumino-silicate fibers doped with Bismuth," Opt. Mater. Express **6**(2), 486–508 (2016).

1. Introduction

Currently, researches aiming development of 'active' (applicable for lasing) optical fibers with low loss in the mid-IR spectral range (*i.e.* at wavelengths over 2 μm) get big deal of attention, being a call of now-a-days applications. Among such applications note laser surgery (*e.g.* 'laser scalpel'), becoming indispensably safe when operating wavelengths are beyond 2 μm, given that human tissues are basically composed of water and hence strongly absorb light, due to intensive absorption bands of OH-groups in this spectral range. Other potential applications of such fibers are coherent mid-IR tomography; telecommunications at 'new' wavelengths (since telecom capacities tend now to saturate at conventional wavelengths, <1.8 μm, thus forcing a search for mid-IR telecom channels where the propagation losses are still low whereas the nonlinear-optical effects become much weaker than in near-IR (NIR), the requirement well matched in the 2…3 μm range), ecology of atmosphere (given that at over 2 μm one of its 'transmittance windows' is located), and optical sensing of ionizing radiations.

Meanwhile, exponential growth of internal loss with wavelength in silica fibers, once it exceeds ~2 μm (due to attenuation on phonons of 'bigger' energy, inherent to this network), severely obstacles assessing the referred applications. In this regard, extensive researches were ongoing towards defining an alternate chemical composition of fiber's core-glass with lowered loss in mid-IR, among which such candidates as fluoride, chalcogenide, telluride, and zirconium-based glasses deserve mentioning: all these glasses demonstrate more relevant phonon spectra than silicates. However, progress in the field is still limited.

The above said explains our motivation to attempt fabricating fibers with core-glass co-doped, in different degree, with Hafnium (Hf) and to characterize them from different points of view. Fibers of this type can be a good choice for mid-IR applications as expectedly having reduced, as compared to standard silica-based ones, effective phonon energy and, thus, reduced fundamental loss in the mid-IR. The idea to develop optical fibers with SiO_2-HfO_2 network of core-glass stems from the known fact that HfO_2 is a material with a high refractive index (RI), transparent over a wide wavelength range, 0.4…6 μm (see *e.g* [1].). We have chosen such kind of core-glass as also promising for high-power laser applications, requiring a high optical-damage threshold: HfO_2 belongs to this class of oxides. Note that in silicates Hf ions are coordinated to more than four oxygen atoms, with creation of non-bridging oxygens (NBOs) in silica network [2]; flexibility of such network seems to be high – given by the presence of NBOs – to allow the host glass to accommodate, in almost equivalent environments, other optically-active in NIR/mid-IR co-dopants (say, rare-earths such as Holmium (Ho) and Erbium (Er) or post-transitional metals such as Bismuth (Bi)) [3]. Note here that the effect of Hf co-doping of rare-earth doped silica fibers has been inspected so far in very few works while found to be mostly positive [4,5]. We also considered that HfO_2 can be capable to modify the overall core-glass structure, facilitating dispersion of 'active' co-dopants. But, on the other hand, the addition of Hf may result in overall inhomogeneity of the glass network to be formed, thus leading to problems in real applications. Clarification of these, hypothetically controverting, appearances of Hf co-doping of silica based fibers, is one of the purposes of the current work.

Below, we provide the fabrication details and optical tests of novel hafnia-yttria-alumina-silicate (further – HYAS) core-glass preforms and fibers, one of which additionally co-doped with Bi. To the best of our knowledge, it is the first report about success in making optical

Optical Materials EXPRESS

fiber of such kind (a sole recent work [6] informing the fabrication of SiOC/HfO_2 ceramic fiber, derived from sol-gel process, deals with quite special type of core-less fiber).

2. Fabrication details and experimental methods

The HYAS core-glass based preforms were fabricated through the Modified Chemical Vapor Deposition (MCVD) process gathered with the Solution Doping (SD) technique, followed by suitable thermal treatment. Note that SiO_2 (and P_2O_5 in small amount) served as glass formers and were incorporated via the MCVD process while the glass modifiers Al_2O_3, HfO_2, and Bi_2O_3 (in case of co-doping with Bi) were added via SD. During SD, soaking of porous soot layers of sourcing tubes was done into solution of alcoholic-water (1:5) mixture, $Al(NO_3)_3$: $9H_2O$, YCl_3: $6H_2O$, and $HfOCl_3$: $8H_2O$ (plus, in case of Bi co-doping, $Bi(NO_3)_3$: H_2O), for ~1 h. After draining out the solution, the core layers were dried with flow of N_2 gas at room temperature and then dried thermally, by heating up to ~500°C with flow of mixture of O_2 and He gases, for oxidizing the salts. Sintering of the layers and collapsing of the tubes were made in atmosphere of the same gases at higher temperatures, 1500…1800°C and 2000…2300°C, respectively. Posteriorly, the preforms were thermally annealed at around 1000°C in a controlled heating furnace, which gave rise to creating HYAS glass of ceramic type in the preforms' core regions. The final HYAS based fibers were drawn from the annealed preforms by a conventional way using a fiber drawing tower, at ~2000°C. All fibers were designed to be multimode, of 125 ± 0.5/11.5 ± 1.5-μm cladding/core diameters and numerical apertures (N.A.) of 0.17…0.23 (see Table 1), for facilitating spectral measurements. Hereafter, we report the results of characterization of three samples of the HYAS core-glass based fibers: HF2, HF3 (without co-doping with any 'active' impurity), and HF4_Bi (co-doped with Bi). Note that concentrations of $HfOCl_3$ in alcoholic-water solutions at SD of preforms HF3 and HF4_Bi were approximately 2 to 3 times bigger than at SD of preform HF2.

Table 1. The fibers' basic parameters

ID	Core composition	Core diameter μm	N.A.	Al_2O_3 mol.%	Y_2O_3 mol.%	HfO_2 mol.%	Bi_2O_3 mol.%
HF2	SiO_2-Al_2O_3-HfO_2-Y_2O_3	10	0.17	3.4	0.05	0.69	---
HF3	SiO_2-Al_2O_3-HfO_2-Y_2O_3	11	0.21	7.2	0.12	2.65	---
HF4_Bi	SiO_2-Al_2O_3-HfO_2-Y_2O_3-Bi_2O_3	13	0.23	6.25	0.05	1.11	0.02

The radial distributions of co-dopants in the HYAS core-glass based fibers were measured using Electron Probe Micro Analysis (EPMA); the experiments were proceeding with short pieces (centimeters) of fiber samples. RI profiles of the fibers were obtained using a fiber analyzer, at 633 nm (HeNe laser). Absorption spectra of fibers (few meters in length) were recorded with optical spectrum analyzers (OSAs) (Yokogawa AQ6370B and Ando 6315A), by the cutback method. Fluorescence spectra of HF4_Bi fiber were obtained using the same OSAs at pumping by laser diodes (Q-Photonics and Innolume) with operational wavelengths 908 and 1120 nm; fluorescence was detected in 'backward' scheme, allowing to filter out the pumps' spontaneous emission remnants. The fluorescence lifetime of HF4_Bi fiber was as well measured in backward geometry but in that case pump-light was modulated by means of an acousto-optical modulator (OptoElectronics, operation frequency, 10 MHz); the backward fluorescence, modulated accordingly, was detected using a photo-detector and oscilloscope (DPO7354C, Tektronix).

3. Results and discussion

A line of techniques was employed to characterize the overall state-of-the-art of the fabricated fibers, useful for further studies and potential applications of this or similar type of fiber.

The EPMA measurements of HF2, HF3, and HF4_Bi fibers gave us the results shown in Fig. 1(a), 1(b), and 1(c), respectively; refer also to Table 1.

Optical Materials EXPRESS

As seen, we were successful in co-doping the fibers with Hf at SD preform-stage, with obtained Hf contents ranging from 0.6 to 2.8 mol.%; see the orange-color radial distributions of HFO_2 in Fig. 1. As seen from the figure and Table 1, the fibers' core-glass has been also co-doped with Al_2O_3 (black curves), Y_2O_3 (magenta curves), and Bi_2O_3 (grey curves) [in HF4_Bi fiber: see Fig. 1(c)]. Note that the oxides' molar contents entered the fibers' core areas are roughly proportional to the salts' contents, soaked into preforms at SD.

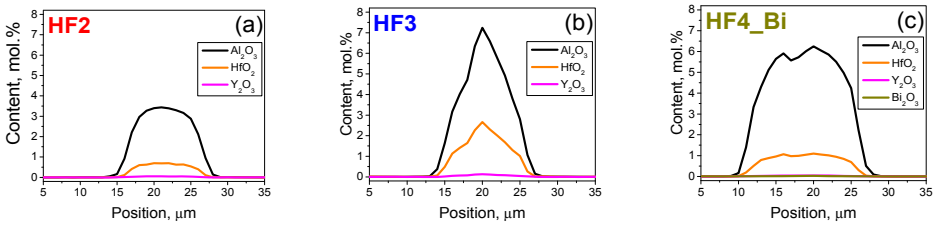

Fig. 1. Distributions of elements constituting core-glasses of HF2 (a), HF3 (b), and HF4_Bi fibers (from the EPMA data).

In Fig. 2 (main frames), we demonstrate the difference attenuation spectra of the HYAS fibers HF2 (a), HF3 (b), and HF4_Bi (c), obtained after subtracting the original loss spectra, collected in their straight and coiled (curvature diameter, 5 cm) positions.

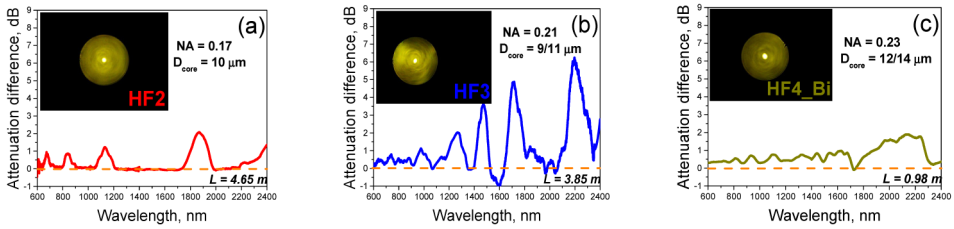

Fig. 2. Main frames: attenuation difference spectra in VIS to mid-IR, obtained for HF2 (a), HF3 (b), and HF4_Bi fibers (lengths of samples L are indicated in the plots' corners). Insets: micro-photographs of cleaved fiber surfaces.

It is seen that all fibers are strongly multimode up to at least 2.4 μm: their different-order cutoffs (seen as peaks in the difference attenuation spectra) span the accessible visible (VIS) to mid-IR spectral range. Notice that, despite of similar core diameters and N.A. of HF2 and HF3 fibers (differed only in Hf concentrations: in HF3 it is a few times bigger than in HF2), the cutoffs appearance is more sophisticated in HF3 than in HF2. Most probably, this is a result of polarization de-genericity of the transversal modes, supported in HF3 fiber (heavier doped with Hf). An argument in support of this statement is (see insets to Fig. 2(a) and 2(b)), demonstrating the microscopic cross-sectional images of the fibers) slight ellipticity of the core-area of HF3 fiber (measured by 9…11 μm in orthogonal directions), as compared to almost circular core region of HF2 fiber (measured by 10 μm). Furthermore, the cutoffs' pattern in case of HF4_Bi fiber (see Fig. 2 (c)), as well heavier doped with Hf than HF2 while additionally co-doped with Bi, is also complicate but less resolved, although its core demonstrates elliptical shaping, too. The revealed features signify that the addition of Hf may result, in case of exceeding some relative molar ratio Hf/Si, in inhomogeneity of the HYAS core-glass network, or even phase-separation and/or nano-structuration, stemming from inconsistency of the sub-lattices formed by Si and Hf ions (as was noted, Hf ions are coordinated to more than four oxygen atoms, in contrast to Si ones).

In Fig. 3, we demonstrate cross-sectional distributions of RI in the core-areas of HF2 (a), HF3 (b), and HF4_Bi (c) fibers. As seen from the plots, quite big RI-differences between the core and cladding regions were established, revealing a big effect of Hf co-doping (despite

Optical Materials EXPRESS

relatively low abundance of Hf ions in the core-glass network; refer to Table 1) on the refractive, and hence wave-guiding, properties of the HYAS based fibers. Thus, the property of HfO_2 being a highly refractory material (see *e.g* [7].) is confirmed by our results on measuring RI in the fibers. Note that the maximal RI-values, *i.e.* the ones measured in central parts of the distributions (n_{core}) were used to plot this quantity in function of HfO_2 molar weight; see the inset to Fig. 6. Also note the sharpness of the RI-profiles across the core region of the fibers (especially, at high Hf-doping, see Fig. 3(b) and 3(c)), observed in contrast to smoother radial distributions of the elements (Al_2O_3 and HfO_2), mainly contributing in RI of the core region (refer to Fig. 1). Possible reasons of such a difference are still unclear and need a separate study in future, but it can be explained by the already hypothesized inhomogeneity of the HYAS core-glass network (through phase-separation and/or nano-structuration) and by the fact [8] that variation of the molar ratio SiO_2/HfO_2 leads to a complicate character (decrease and increase) of the RI of the mixed material (in our case, the presence of Al_2O_3 can only sophisticate the situation).

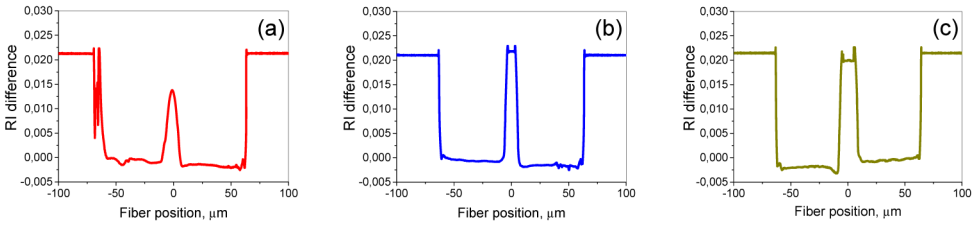

Fig. 3. RI profiles of HF2 (a), HF3 (b), and HF4_Bi (c) fibers.

In Fig. 4, we show the attenuation spectra of fibers HF2, HF3, and, for comparison, commercial Hf-free alumina-silicate smf-28 fiber, obtained for the mid-IR (1950…2400 nm) (a) and VIS to NIR (500…1400 nm) (b) ranges, respectively. As seen from Fig. 4(a), the addition of Hf (in HF2 and HF3 fibers) merely reduces the losses in the mid-IR as compared to smf-28 fiber, by ~3.5…4 times, at wavelengths exceeding 2 μm. This reveals a clue role of Hf co-doping in diminishing attenuation in this spectral range, which is the main result of the present work, deserving attention.

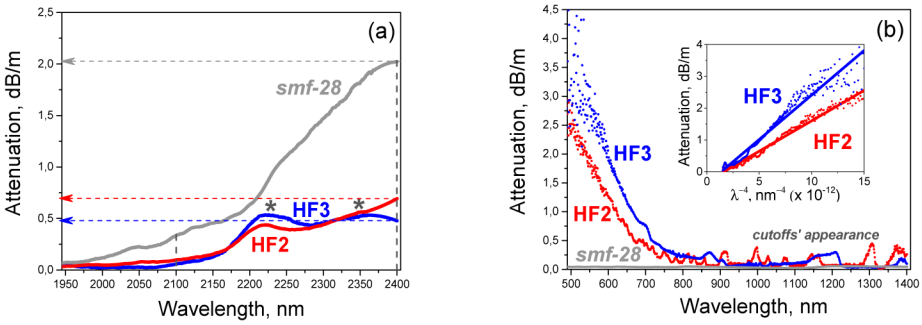

Fig. 4. Attenuation spectra of HF2 (red), HF3 (blue), and smf-28 (gray) fibers measured in mid-IR (>2 μm) (a) and VIS to NIR (b) regions. In (a), arrows specify attenuations at wavelengths 2.1 and 2.4 μm, used to build the dependences shown in Fig. 5, and asterisks mark the spectral positions of loss produced by OH-related centers. In (b), inset shows the same dependences as those plotted in main frame but re-scaled *vs.* λ^{-4} (solid lines are linear fits of the data), thus indicating a law characteristic to Rayleigh scattering, for both fibers.

Furthermore, the smooth peaks in the attenuation spectra of these two fibers (asterisked in (a)), are produced by centers associated with hydroxyl (OH^-) groups, given that these groups are inevitably present in core-glass because of the method employed at the fibers' manufacturing. Remind that these two, as well as HF4_Bi fiber, were made at SD soaking

Optical Materials EXPRESS

from water/alcohol solution. Our estimates show that OH^- content in our fibers is 1.5 ± 0.4 ppm (the data were obtained after averaging of loss values in OH^- peaks @1.38 and @2.24 μm).

On the other hand, as seen from main frame of Fig. 4(b), HF2 and HF3 fibers both suffer notable rise of attenuation in VIS towards ultraviolet (UV), the behavior indicating an increase of scattering loss (see inset to the figure); noteworthy, nothing resembling this happens with 'standard' (Hf-free) smf-28 fiber. Seemingly, this phenomenon, stemming from co-doping with Hf, can be explained by already mentioned phase-separation in this (HYAS) type of core-glass [a similar effect arises in Bi co-doped HF4_Bi fiber, see Fig. 5(a)], a disadvantage that arises 'in expense' of the advantage being overall decreasing of loss at >2 μm (Fig. 4(a)). On the other hand, some contribution in attenuation in VIS of the fibers can be produced by NBOs, formed in a big amount, as was mentioned above, at co-doping silica glass with Hf. Also, note that the small peaks in the attenuation spectra of HF2 and HF3 fibers (Fig. 4(b)) adhere to the fibers' multimode nature, being nothing than cutoff peaks (Fig. 2).

In the main frame of Fig. 5(a), we show the attenuation spectrum of HF4_Bi fiber. It is seen that, as in cases of HF2 and HF3 fibers, there is an increase of scattering towards shorter wavelengths, hypothetically indicating phase-separation and/or nano-structuration of their core-glass due to co-doping with Hf and Bi. However, in contrast to HF2 and HF3 fibers, HF4_Bi fiber demonstrates the characteristic absorption bands within the 400…1400 nm range, thus apparently signifying the presence of fluorescence-active centers, associated with Bi (so-called BACs), marked by arrows. [The peak at ~1400 nm reveals the loss produced by OH-groups.] Note that the spectral positions of Bi-related absorption bands (absent in HF2 and HF3 fibers) resemble the ones referred to as BACs:Al in alumina-silicate Hf-free fibers [7–10]. Furthermore, see inset to Fig. 5(a), the attenuation spectrum of HF4_Bi fiber in the mid-IR (1900…2400 nm) demonstrates, as in case of HF2 and HF3 fibers, overall reduction of the phonon-related loss (as compared to smf-28 fiber) by ~4 times, as well due to Hf co-doping. Note that the smooth (asterisked in the inset) peaks are indicative of the presence of OH-related centers (compare with Fig. 2(a)) while the peak at ~2000…2050 nm is provisionally considered to be produced by Bi-related centers, because in Bi-free HF2 and HF3 fibers such feature is not detected.

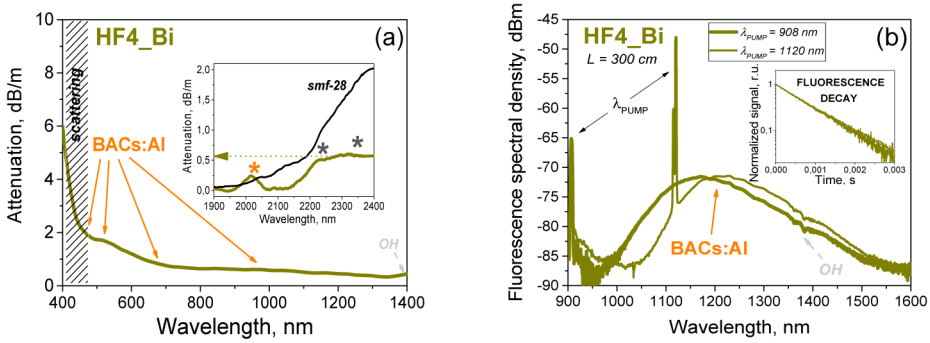

Fig. 5. (a) Attenuation spectrum of HF4_Bi fiber, measured in VIS/NIR (400…1400 nm) (main frame) and at >2 μm (inset); in inset, black-color asterisks mark the spectral contributions in attenuation of OH-related centers and black curve copies from Fig. 4(a) the absorption spectrum of smf-28 fiber. (b) Fluorescence spectra of HFBi_4 fiber obtained at 908 and 1120 nm excitations (main frame) and (inset) decays of the normalized NIR fluorescence signals, detected at pumping the fiber at these wavelengths). In both panels, orange arrows specify the spectral positions of the resonant-absorption (a) and fluorescence (b) bands of BACs.

We also checked the fluorescent ability of HF4_Bi fiber at excitation at the wavelengths falling into one of the resonant-absorption bands of BACs, near ~1 μm: @908 and @1120

Optical Materials EXPRESS

nm; see main frame of Fig. 5(b); launched power in both pump conditions was around 150 mW. It is seen that HF4_Bi fiber demonstrates intensive broadband, 1000…1600-nm, fluorescence, similarly to NIR fluorescence characteristic to Bi-doped alumina-silicate Hf-free fibers; hence, it is produced by BACs:Al, with no or little effect given by Hf co-doping.

Furthermore, our measurements of the NIR fluorescence decay have shown (see inset to Fig. 5(b)) that it obeys the exponential law, at both kinds of excitation. Fitting of the decays gave the NIR fluorescence lifetime of ~1.1 ms, which is close but a bit bigger than that known for Hf-free alumina-silicate Bi-doped fibers (see e.g [9–12].). Thus, the results presented in Fig. 5(b) may evidence for good potential of such-type fibers for lasing/amplifying in NIR, as mentioned in Section 1.

In Fig. 6, we provide overview of the results of mid-IR attenuation measurements in all fibers with the HYAL core-glass, *i.e.* HF2, HF3, and HF4_Bi, as compared to smf-28 fiber, exemplified by losses at two wavelengths, 2.1 and 2.4 μm. It is seen that increasing degree of co-doping with Hf (counted here in terms of Hf-content in final fibers; see Table 1) apparently results in considerable lowering of the mid-IR loss; as for us, it is a meaningful result.

Note that minimizing loss at 'operational' wavelengths of, say, Ho-doped fiber lasers (~2.0…2.2 μm) is a hot topic now; hence, usage of Hf/Ho co-doped fibers may be a proper solution for 2-μm lasing or amplifying.

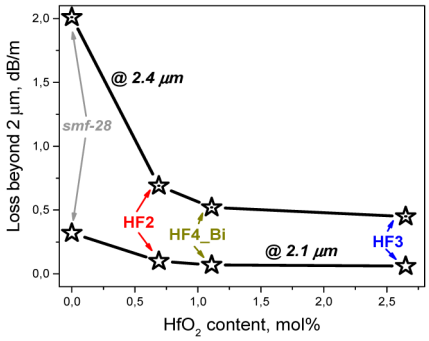

Fig. 6. Dependences of mid-IR loss, exemplified for wavelengths 2.1 and 2.4 μm, on HfO_2 molar content, in HF2, HF3, and HF4_Bi fibers, in comparison with smf-28 fiber (zero co-doping with Hf level in X-scale).

Consider the data, useful for further improvements, of our experiments on drawing fiber Bragg gratings (FBGs) in the HYAS core-glass based fibers, Fig. 7.

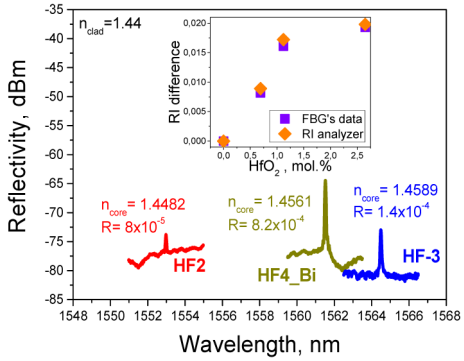

Fig. 7. Main frame: Spectral reflection on FBGs inscribed in Hf2, HF3, and HF4_Bi fibers (with the values of n_{core} and absolute reflectivity R being provided near each spectrum). Inset: the dependence of RI-difference between the core and cladding areas on HfO_2 molar content.

Optical Materials EXPRESS

In main frame of the figure, we demonstrate the reflection spectra of FBGs, inscribed in the fibers under the action of UV (244-nm, 75 mW) irradiation, employing a mask with a 536.194-nm pitch, during the same irradiation time (40 min.). The values of reflectivity (R) accessed in maxima of the spectra and n_{core} (RI of core areas) are indicated in the figure. It deserves attention that, at increasing Hf-content in the core-glass (in a 'row' HF2 → HF4_Bi → HF3; see the colored spectra), a noticeable change (*viz.*, increase) in RI-difference is maintained. This dependence, specified in terms of Hf-content, is demonstrated in inset to Fig. 7 by violet squares. For comparison, in the same plot, we provide (by orange rhombs) the RI-difference data obtained using RI-analyzer (refer to Fig. 3). Remarkably, both the dependences are nearly identical, thus ensuring validity of the results (obtained, note, using the completely different measurement methods).

Resuming, the data shown in Fig. 7 (a strong change of core-RI with increasing Hf-doping level into silica network) force us to reveal a considerable modification of the core-glass through addition of Hf, which agrees well with the other feature, already discussed, *viz.* diminishing of the mid-IR loss beyond 2 μm (refer to Figs. 4–6).

4. Conclusions

We reported fabricating of a set of multimode hafnia-yttria-alumina-silicate (HYAS) core-glass based fibers, one of which co-doped with Bismuth (Bi), for the mid-IR (> 2 μm) range.

We showed that the Conventional Modified Chemical Vapor Deposition (MCVD) method in conjunction with Solution Doping (SD) technique employed for the fibers manufacturing guarantees success in co-doping core-glass with Hafnium (Hf) in contents (up to a few mol.%) suitable for considerable (a few times) lowering of the fundamental loss beyond 2 μm, as compared to Hf-free silica fiber. This advantage indicates possible usefulness of fibers of this or similar type for versatile mid-IR applications. On the other hand, a disadvantage of the HYAS-glass fibers, established at the current stage of our work, is that addition of Hf in the realized concentrations leads to an increase of scattering, seen as growth of loss towards shorter wavelengths, which may be indicative of phase separation or nano-structuration of the core-glass. Moreover, co-doping with Hf in amounts exceeding 0.7…0.8 mol.% (HfO_2) results in loosing concentricity of the core-area, probably because of inhomogeneity of its network through inconsistency of the sub-lattices formed by Si and Hf atoms, given that Hf atoms (much bigger in size) are known to coordinate to more than four oxygen atoms, unlike Si ones, which leads to formation of non-bridging oxygens in a big amount. Furthermore, we demonstrated that a version of HYAS core-glass fiber co-doped with Bi reveals all signs in absorption and fluorescence spectra it possesses, stemming from the presence of 'active' Bi centers (BACs), associated with Al. Seemingly, such type of fluorescence-active Hf/Bi co-doped fiber may be suitable for lasing/amplifying and other applications in the near-IR.

One of the current study's result is a demonstration of the new method of inscribing fiber Bragg gratings and their analysis for indirect but reliable measurement of refractive index of core-glass of an optical fiber.

Finally note that, despite of moderate success of the current study, a line of future works to fabricate Hf co-doped fibers with improved optical characteristics is certainly required. Among them, it seems natural to employ other techniques to fabricate such fibers (e.g. Direct Nanoparticle Deposition to avoid SD soaking), aiming farther decreasing mid-IR loss, *viz.* its part associated with OH^- groups presence, inherent to the 'combined' MCVD/SD technique.

Funding

Financial support through the Indo-Russian Cooperative Program (Project #15-52-45024, RFBR, Russia, and DST, India); the Increase Competitiveness Program of NUST «MISiS» (#K3-2017-015) of the Ministry of Education and Science of the Russian Federation; and the Consejo Nacional de Ciencia y Tecnologia (CONACyT, Project #242221) is acknowledged.